PROCEEDINGS OF SPIE

Infrared, Millimeter-Wave, and Terahertz Technologies II

Cunlin Zhang
Xi-Cheng Zhang
He Li
Sheng-Cai Shi
Editors

5–7 November 2012
Beijing, China

Sponsored by
SPIE • COS—Chinese Optical Society

Cooperating Organizations
Tsinghua University (China) • Peking University (China) • Zhejiang University (China) • Beijing Institute of Technology (China) Beijing University of Posts and Telecommunications (China) • University of Science and Technology of China (China) Tianjin University (China) • Nankai University (China) • Changchun University of Science and Technology (China) • University of Shanghai for Science and Technology (China) • Capital Normal University (China) • Huazhong University of Science and Technology (China) • Beijing Jiaotong University (China) • Shanghai Institute of Optics and Fine Mechanics (China) Changchun Institute of Optics and Fine Mechanics (China) • Institute of Semiconductors (China) • Institute of Optics and Electronics (China) • National Univ. of Defense Technology (China) • Institute of Physics (China) • Shanghai Institute of Technical Physics (China) • China Instrument and Control Society (China) • Optoelectronics Technology Committee, COS (China) • SPIE National Committee in China (China) • Japan Optical Society (Japan) • Korea Optical Society (Korea, Republic of) • Australia Optical Society (Australia) • Singapore Optical Society (Singapore)

Supporting Organizations
CAST—China Association for Science and Technology (China) • NSFC—National Nature Science Foundation (China)

Published by
SPIE

Volume 8562

Proceedings of SPIE 0277-786X, V.8562

Infrared, Millimeter-Wave, and Terahertz Technologies II, edited by Cunlin Zhang, Xi-Cheng Zhang, He Li, Sheng-Cai Shi, Proc. of SPIE Vol. 8562, 856201 · © 2012 SPIE · CCC code: 0277-786/12/$18 · doi: 10.1117/12.2018523

Please use the following format to cite material from this book:
Author(s), "Title of Paper," in *Infrared, Millimeter-Wave, and Terahertz Technologies II*, edited by Cunlin Zhang, Xi-Cheng Zhang, He Li, Sheng-Cai Shi, Proceedings of SPIE Vol. 8562 (SPIE, Bellingham, WA, 2012) Article CID Number.

ISSN: 0277-786X
ISBN: 9780819493170

Published by
SPIE
P.O. Box 10, Bellingham, Washington 98227-0010 USA
Telephone +1 360 676 3290 (Pacific Time) · Fax +1 360 647 1445
SPIE.org

Printed in the United States of America.

Publication of record for individual papers is online in the SPIE Digital Library.

SPIE Digital Library

SPIEDigitalLibrary.org

Paper Numbering: Proceedings of SPIE follow an e-First publication model, with papers published first online and then in print and on CD-ROM. Papers are published as they are submitted and meet publication criteria. A unique, consistent, permanent citation identifier (CID) number is assigned to each article at the time of the first publication. Utilization of CIDs allows articles to be fully citable as soon as they are published online, and connects the same identifier to all online, print, and electronic versions of the publication. SPIE uses a six-digit CID article numbering system in which:

- The first four digits correspond to the SPIE volume number.
- The last two digits indicate publication order within the volume using a Base 36 numbering system employing both numerals and letters. These two-number sets start with 00, 01, 02, 03, 04, 05, 06, 07, 08, 09, 0A, 0B … 0Z, followed by 10-1Z, 20-2Z, etc.

The CID Number appears on each page of the manuscript. The complete citation is used on the first page, and an abbreviated version on subsequent pages. Numbers in the index correspond to the last two digits of the six-digit CID Number.

Contents

POSTER SESSION

Symposium Committees

General Chairs

Eustace L. Dereniak, College of Optical Sciences, The University of Arizona (United States)
Bingkun Zhou, Tsinghua University (China)

General Cochairs

Arthur Chiou, National Yang-Ming University (Taiwan, China)
Zhizhan Xu, Shanghai Institute of Optics and Fine Mechanics (China)
Jianlin Cao, China Ministry of Science and Technology (China)
Junhao Chu, Shanghai Institute of Technical Physics (China)

Technical Program Chairs

Songlin Zhuang, Shanghai University of Science and Technology (China)
Xingde Li, Johns Hopkins University (United States)

Technical Program Cochairs

Qiming Wang, Institute of Semiconductors (China)
Xu Liu, Zhejiang University (China)
Daoyin Yu, Tianjin University (China)
Qihuang Gong, Peking University (China)
Tianchu Li, National Institute of Metrology (China)
Wei Huang, Nanjing University of Posts and Telecommunications (China)

Local Organizing Committee Chair

Guangcan Guo, University of Science and Technology of China (China)

Local Organizing Committee Cochairs

Guoqiang Ni, Beijing Institute of Technology (China)
Shusen Xie, Fujian Normal University (China)
Xiaomin Ren, Beijing University of Posts and Telecommunications (China)
Ying Gu, PLA General Hospital (China)
Huilin Jiang, Changchun University of Science and Technology (China)

General Secretary

Qihuang Gong, Peking University (China)

Local Organizing Committee

Yan Li, Chinese Optical Society/Peking University (China)
Zhiping Zhou, Peking University (China)
Changhe Zhou, Shanghai Institute of Optics and Fine Mechanics (China)
Qingming Luo, Huazhong University of Science and Technology (China)
Chongxiu Yu, Beijing University of Posts and Telecommunications (China)
Hongda Chen, Institute of Semiconductors (China)
Yongtian Wang, Beijing Institute of Technology (China)
Yiping Cui, Southeast University (China)
Xuping Zhang, Nanjing University (China)
Feijun Song, Daheng Corporation (China)
Cunlin Zhang, Capital Normal University (China)
Yanting Lu, Nanjing University (China)
Yuejin Zhao, Beijing Institute of Technology (China)
Chunqing Gao, Beijing Institute of Technology (China)
Tiegen Liu, Tianjin University (China)
Xiaocong Yuan, Nankai University (China)
Weimin Chen, Chongqing University (China)
Zhongwei Fan, Academy of Optoelectronics (China)
Hanyi Zhang, Tsinghua University (China)
Lan Wu, Zhejiang University (China)
Yongsheng Zhang, University of Science and Technology of China (China)
Hong Yang, Peking University (China)
Xiaoying Li, Tianjin University (China)
Lin Zhai, Chinese Optical Society (China)

Conference Committee

Conference Chairs

Cunlin Zhang, Capital Normal University (China)
Xi-Cheng Zhang, University of Rochester (United States)
He Li, Shanghai Institute of Technical Physics (China)
Sheng-Cai Shi, Purple Mountain Observatory (China)

Conference Program Committee

Peter A. Ade, Cardiff University (United Kingdom)
Yi Cai, Kunming Institute of Physics (China)
Hou-Tong Chen, The Center for Integrated Nanotechnologies (United States)
Yuping Cui, Jinhang Institute of Technical Physics (China)
Haewook Han, Pohang University of Science and Technology (Korea, Republic of)
Weiqi Jin, Beijing Institute of Technology (China)
Ci-Ling Pan, National Tsing Hua University (Taiwan, China)
Jiancheng Shi, Institute of Remote Sensing Applications (China)
Alexander Pavlovich Shkurinov, Lomonosov Moscow State University (Russian Federation)
Masahiko Tani, University of Fukui (Japan)
Chao Zhang, University of Wollongong (Australia)
Yan Zhang, Capital Normal University (China)

Session Chairs

1 Session 1
Cunlin Zhang, Capital Normal University (China)

2 Session 2
Cunlin Zhang, Capital Normal University (China)

3 Session 3
Xi-Cheng Zhang, University of Rochester (United States)

4 Session 4
Xi-Cheng Zhang, University of Rochester (United States)

5 Session 5
Sheng-Cai Shi, Purple Mountain Observatory (China)

6 Session 6
Guozhong Zhao, Capital Normal University (China)

7 Session 7
Jingling Shen, Capital Normal University (China)

8 Session 8
Jingling Shen, Capital Normal University (China)

Quantum dot lasers and relevant nanoheterostructures

Alexey E. Zhukov*[a], Natalia V. Kryzhanovskaya[a], Artem V. Savelyev[a], Alexey M. Nadtochiy[a], Ekaterina M. Arakcheeva[a], Fedor I. Zubov[a], Vladimir V. Korenev[a], Mikhail V. Maximov[b], Yuri M. Shernyakov[b], Marina M. Kulagina[b], Ilia A. Slovinskiy[b], Daniil A. Livshits[c], Alexandros Kapsalis[d], Charis Mesaritakis[d], Dimitris Syvridis[d], Alexander Mintairov[e]

[a]St. Petersburg Academic University, Khlopina 8(3), St Petersburg, Russia 194021; [b]Ioffe Physical-Techical Institute, Politekhnicheskaya 26, St Petersburg, Russia 194021; [c]Innolume GmbH, Konrad-Adenauer-Allee 11, Dortmund, Germany 44263; [d]University of Athens, Athens, Greece 15784; [e]University of Notre Dame, 275 Fitzpatrick Hall, Notre Dame, IN 46556, USA

ABSTRACT

Spectral and power characteristics of QD stripe lasers operating in two-state lasing regime have been studied in a wide range of operation conditions. It was demonstrated that neither self-heating nor increase of the homogeneous broadening are responsible for quenching of the ground-state lasing beyond the two-state lasing threshold. It was found that difference in electron and hole capture rates strongly affects light-current curve. Modulation *p*-type doping is shown to enhance the peak power of GS lasing transition. Microring and microdisk structures (D = 4–9 µm) comprising 1.3 µm InAs/InGaAs quantum dots have been fabricated and studied by µ-PL and NSOM. Ground-state lasing was achieved well above root temperature (up to 380 K). Effect of inner diameter on threshold characteristics was evaluated.

Keywords: Quantum dots, semiconductor laser, microring resonator, two-state lasing

1. INTRODUCTION

For various applications, including optical data transmission, pumping of Raman amplifiers, aesthetic laser surgery, etc, efficient lasers operating around 1.3 µm are requested. Lasers based on self-organized InAs/InGaAs quantum dots (QDs) offer an attractive combination of the required wavelength with extremely low threshold current density and high characteristic temperature. However, at sufficiently high currents a shorter-wavelength ($\lambda \sim 1.2$µm) band caused by the first excited-state (ES1) transition appears in the spectrum[1]. Such a behavior is now referred to as two-state lasing. For a majority of applications two-state lasing has to be suppressed whereas the GS spectral component of the lasing spectrum has to be maximized. Analysis of QD laser behavior based on rate[2] and master[3] equations predicts that optical power of the GS component reaches its maximal value at threshold of the two-state lasing and then persists. However a number of experimental facts revealed that the GS component declines down to its complete quenching[4,5] due probably to laser self-heating in CW regime[4] and/or increase of homogeneous broadening[5] have been proposed. To clarify possible reasons of the GS lasing quenching we studied spectral and light-current characteristics of broad-area QD lasers.

Microdisks and microrings optical resonators comprising a III-V active region are promising candidates for light emitters to be integrated with silicon photonic circuits. Owing to a combination of a compact size and a high Q-factor, which can be achieved in such structures, ultralow threshold operation is expected. Although the majority of whispering gallery mode (WGM) resonators has been contained quantum-well active region composed of InP-based materials[6], QDs may have certain advantages. These include attainability of 1.3 µm emission in GaAs-based structures with high refractive index contrast, low temperature sensitivity, suppressed sidewall recombination rates[7], making it possible to achieve lasing in resonators of small diameter. Since the first report[8] on QD microdisk laser capable of operating at 77K, significant progress has been made toward high-temperature lasing. In particular, room-temperature lasing has been reported to date for microdisks of few microns in diameter[9], whereas for relatively large microrings (35-85 µm) lasing has been recently extended up to 50°C[10]. In the present work we demonstrate ground-state lasing up to 107°C for optically pumped microring lasers (MRLs) having an outer diameter as small as 6-7 µm.

*zhukale@gmail.com; phone 7 812 4488594; fax 7 812 4486994; www.spbau.ru

Semiconductor Lasers and Applications V, edited by Ning Hua Zhu, Jinmin Li, Frank H. Peters, Changyuan Yu,
Proc. of SPIE Vol. 8552, 855202 · © 2012 SPIE · CCC code: 0277-786/12/$18 · doi: 10.1117/12.2009055

2. TWO-STATE LASING AND ITS SUPPRESSION IN QD LASERS

2.1 Quenching of GS spectral component

Epitaxial structures comprising a single plane or multiple planes of InAs/InGaAs QDs were grown by molecular beam epitaxy. Stripe lasers of various cavity lengths were tested in pulse regime (300ns @ 2 kHz) on temperature-stabilized heatsink. An evolution of the lasing spectrum with increasing the pump current is shown in Figure 1,a for a 4-mm-long single-QD-plane laser at 17^{o}C. The corresponding light-current characteristics (total output power and optical power of GS and ES1 spectral components of the spectrum) are presented in Figure 1,b. The ES1 band (around 1.18 μm) appears in the spectrum at approximately 3 A whereas the GS component reaches its maximum at 5A, well beyond the onset of two-state lasing. A complete quenching of the GS lasing is observed at 12 A.

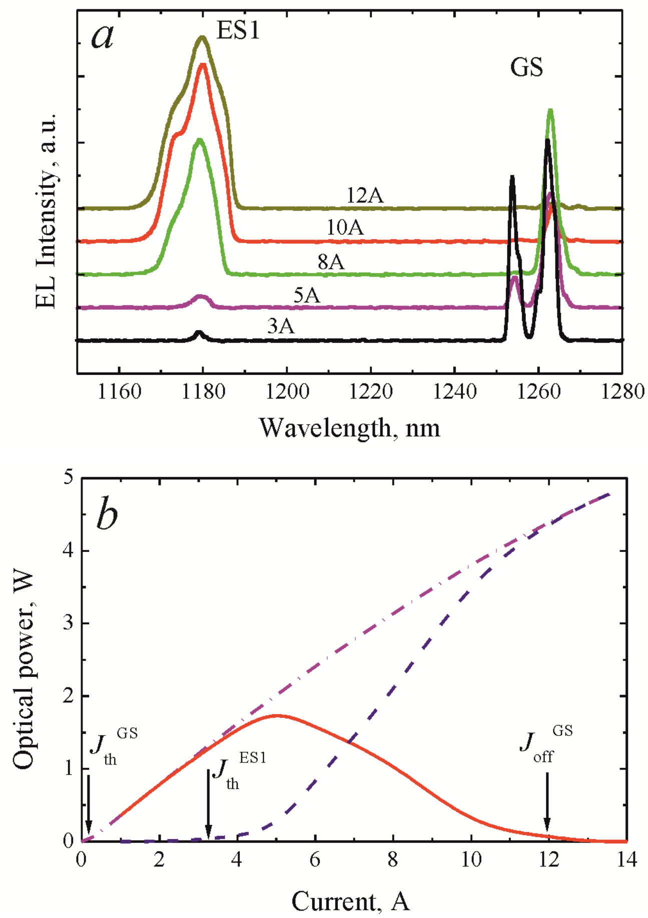

Figure 1. Lasing spectra at different currents (a); laser power (b): dashed-dotted curve – total (GS+ES1), solid curve – ground-state component (GS), dashed curve – first excited-state component (ES1).

As it is seen in Figure 1,a the GS band is split into two peaks (~1.254 and ~1.262 nm). According to M. Sugawara et al[5] this splitting can be attributed to the homogenous broadening of the QD optical transition. They also suggested that the GS lasing quenching at high currents could be explained by increase of the homogenous broadening. In spite of this we found that the splitting is practically unchanged (6.5 $\pm$ 0.4 meV) as current increases up to 12 A. Therefore, the quenching can not be associated with the aforementioned reason. Moreover, spectral positions of the both GS peaks also remain very stable so that the current-induced red shift is only 0.4 nm. Such a shift corresponds to a negligible temperature increment of about 1^{o}C which can not itself lead to suppression of the GS lasing because in this particular laser diode the GS lasing at low currents can be observed up to 68^{o}C. Thus, the GS lasing quenching at high currents can not be attributed to self-heating of the active region as well.

2.2 Effect of difference in electron and hole relaxation rates

More sophisticated model that does not imply either the homogeneous broadening or self-heating effect is based on assumption of the asymmetry in charge carrier distribution in a QD[11]. Energy separation of ground- and excited-state energy levels of holes is much smaller than *kT* that leads to a nearly equal probability of occupation of the hole levels. As a result, there is a competition for the “joint holes” between electrons of the ground-state and the excited-state levels. Because the ES1 electron level has a higher degeneracy as compared to the GS level, in the regime of two-state lasing the holes are effectively swept out from QDs because of their recombination with ES1 electrons. In its turn this leads to the quenching of the GS lasing as the pump current grows.

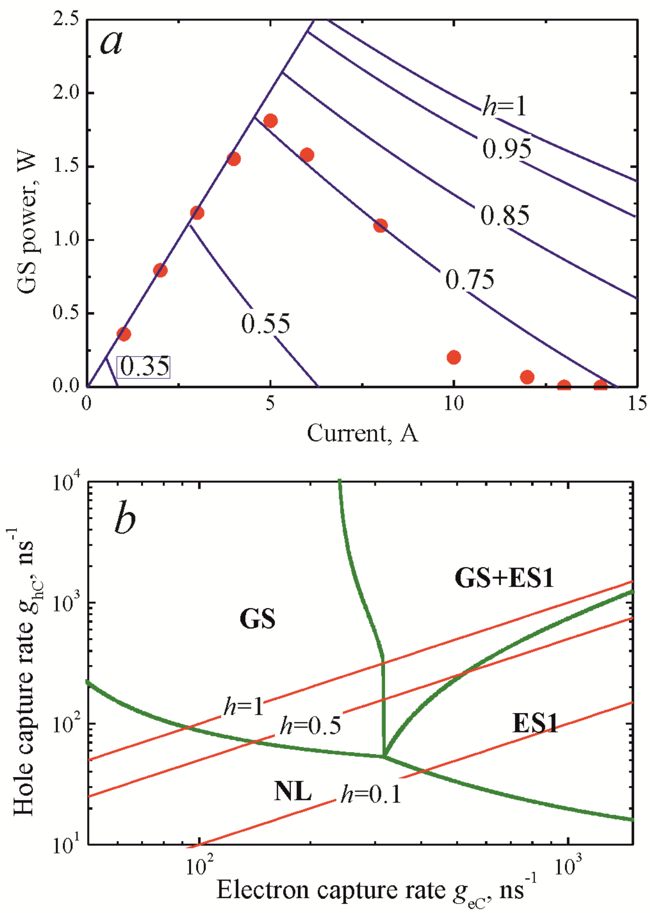

Figure 2. *L-I* curves for ground-state component (a): circles – experiment; lines – calculation for different ratio of hole-to-electron relaxation rates (*h*). Operation diagram of QD laser: heavy lines separates regions of different lasing regimes (NL – no lasing, GS – pure ground-state lasing, GS+ES1 – two-state lasing, ES1 – pure excited-state lasing); thin lines correspond to different *h* values.

However, we found that the observed experimental data can not be quantitatively described if one takes into account only the above-mentioned asymmetry. Reasonable agreement between modeling results and experiment was achieved under assumption that electron and hole relaxation rates into QDs are different. More precisely, we assumed that the hole capture is slower than the electron one which makes the competition for holes more pronounced and leads to complete quenching of the GS lasing at lower pumps. Figure 2,a shows the calculated evolution of the GS power with the pump current. The results are shown for different ratio of the hole-to-electron relaxation rates *h* which is assumed to be independent of the injection rate. The best agreement of the model results with the experiment is found for $h = 0.75$. Lower rate of the hole relaxation is probably associated with their slower velocity in the matrix/wetting layer. Using the extracted value of h we can also reproduce fairly well temperature dependences of the two-state lasing threshold and the current of the GS-lasing quenching.

Using the proposed model we are capable of calculating the operation diagram of QD laser as shown in Figure 2,b. The diagram depicts different regimes of the laser operation as a function of electron (g_{eC}) and hole (g_{hC}) capture rates: subthreshold regime of no lasing (NL), regime of lasing via GS optical transition (GS), two-state lasing regime (GS+ES1), regime of lasing via ES1 transition only (ES1). Depending on the ratio of hole-to-electron relaxation rates ($h = g_{hC}/g_{eC}$) and the total optical loss various scenarios of laser behavior can be realized. In particular, in case of sufficiently fast hole capture ($h = 1$ in Figure 2,b) the two-state lasing can persist so that the GS lasing peak is not completely suppressed even at very high injection levels.

2.3 Effect of *p*-type doping

Modulation *p*-type doping of QDs may noticeably improve temperature stability of the threshold current[12]. We found that *p*-doping affects the two-state lasing behavior as well. Temperature dependences of the two-state lasing threshold current as well as the ground-state lasing threshold current are presented in Figure 3 for two 0.6-mm-long diodes of similar design (10 planes of InAs/InGaAs QDs): one with undoped active region and another with modulation doping (~10 acceptors per QD). The GS-lasing thresholds measured at room temperature are nearly equal in both structures (~0.35 A). At the same time, the onset of the two-state lasing is significantly shifted to higher currents in the *p*-type doped laser (~5.5 A) as compared to its undoped analogue (~1.1 A). Light-current curve (insert of Figure 3) demonstrates that the maximum optical power of the GS spectral component reaches 3.6 W in the laser with *p*-type doping, while it is about 2.4 W in the undoped counterpart. Another finding is that the temperature interval, where GS lasing can be achieved, extends to higher temperatures in the *p*-doped structure (from 55 to 100°C).

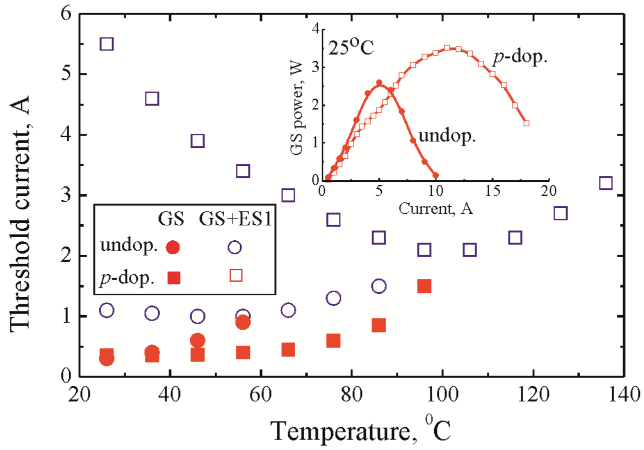

Figure 3. Threshold *vs* temperature for ground-state lasing (solid symbols) and two-state lasing (open symbols) in lasers with undoped (circles) and *p*-type doped (squares) QDs. Insert: power of the GS-line *vs* current.

2.4 Comparison of lasing and spontaneous emission spectra

Spontaneous emission spectra may provide additional information on peculiarities of the two-state lasing. We studied QD lasers having 4 cleaved facets where both lasing and spontaneous emission can be simultaneously detected as shown in Figure 4. At least five peaks of different origin are easily resolved: two narrow peaks of lasing emission via ground-state (1264.3 nm) and first excited-state (1179.8 nm) transitions and three broad peaks of spontaneous emission via ground-state (1264.0 nm), first excited (1172.0 nm) and second excited-state (1108.4 nm) transitions. The characteristic feature is that the GS lasing peak nearly coincides with the peak position of GS spontaneous emission. This implies that the GS lasing arises from QDs of the most probable (mean) size. At the same time ES1 lasing peak is noticeably red-shifted with respect to the peak position of ES1 spontaneous emission indicating that QDs, which size is larger than the mean one, are chiefly responsible for the ES lasing. Similar behavior was observed in a wide interval of current density.

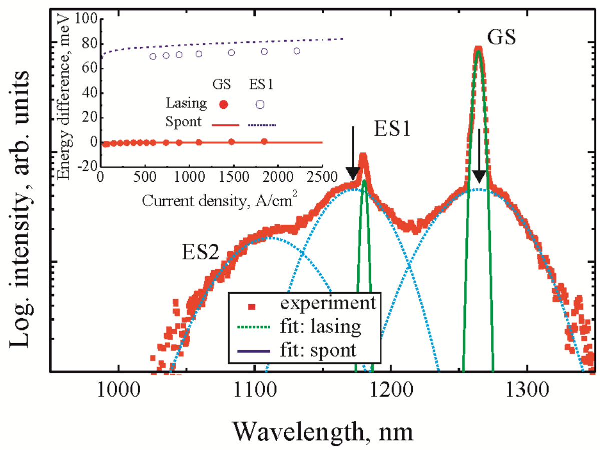

Figure 4. Emission spectrum: squares – experiment, solid curves – lasing emission, dotted curves – spontaneous emission. Insert: peak position *vs* current density: solid circles – GS lasing, open circles – ES1 lasing, solid curve – GS spontaneous emission, dotted curve – ES1 spontaneous emission.

3. MICRORING STRUCTURES

3.1 Experiment

An epitaxial structure was grown by molecular beam epitaxy on semi-insulating GaAs(100) substrate. An active region comprises five layers of $InAs/In_{0.15}Ga_{0.85}As$ QDs separated by 30-nm-thick GaAs spacers. The active region was inserted into a 220-nm-thick GaAs waveguiding layer confined by 20-nm-thick $Al_{0.3}Ga_{0.7}As$ barriers. A 400-nm-thick $Al_{0.98}Ga_{0.02}As$ cladding layer was grown beneath the waveguiding layer. Microrings were defined by photolithography and Ar^+-etching. The outer diameter was varied in different structures from $D = 4$ to 9 µm. The inner diameter ranges from $d = 0$ (microdisks) to $d \approx 0.8D$. Finally, the cladding layer was selectively oxidized into $(AlGa)_xO_y$. Typical microphotograph of the resonator structure is shown in Figure 5.

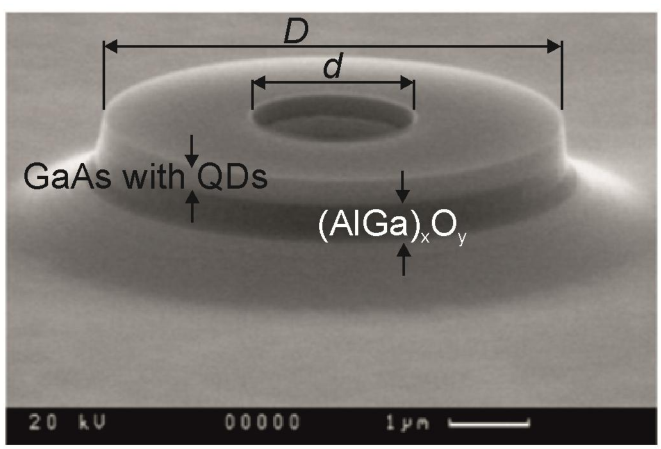

Figure 5. SEM image of QD microring laser (D =6 µm, d = 2 µm).

For optical experiments a CW-operating YAG:Nd laser ($\lambda = 532$nm) was used together with a cooled Ge *pin*-diode. Measurements at elevated temperatures were performed with the structures mounted onto a heated holder equipped with a temperature controller. Low temperature measurements were done in a flow cryostat.

3.2 Low-temperature measurements

An example of luminescence spectrum taken at 77 K from 6μm-ring with 2μm inner diameter is shown in Figure 6. Four series of whispering gallery modes of different radial order are clearly observed. All modes presented in the optical spectrum were identified by means of 2D-axisymmetric analysis. The dominant modes are of $n = 2$ and 3 order. Significant overlap of many modes exists (e.g. around 1190.8 nm where 3 modes are close together).

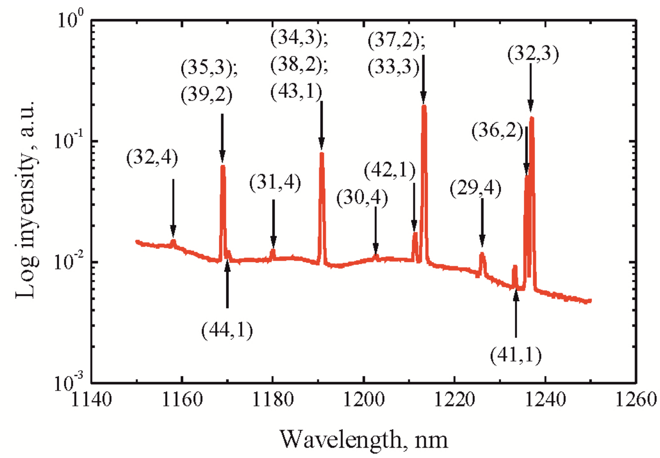

Figure 6. Low-temperature luminescence spectrum of the microring. Estimated mode orders $TE_{m,n}$ are indicated near the peaks.

3.3 Near-field scanning optical microscopy.

Spatial distribution of light intensity inside the microresonators was studied by means of near-field scanning optical microscopy (NSOM). Several typical NSOM images are presented in Figure 7. Characteristic WGM patterns are clearly seen. Depending on spectral position of the luminescence peaks, NSOM images reveal modes of different radial and azimuthal order.

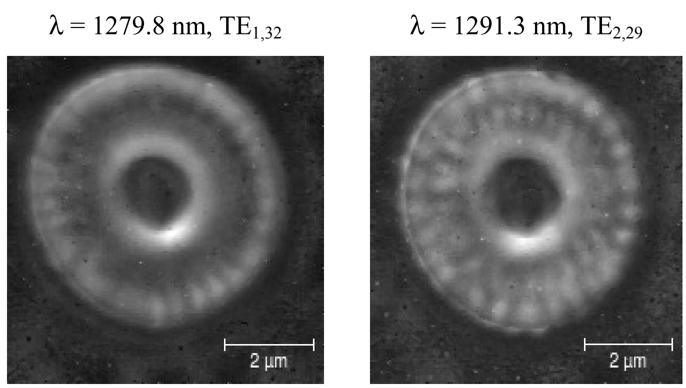

Figure 7. NSOM images demonstrating WGM modes of different orders in the microring resonator.

3.4 Room-temperature measurements.

A representative room-temperature μ-PL spectrum taken under low excitation is shown in the left insert of Figure 8. Full width at half maximum for resonant peaks varies from 0.143 to 0.234 nm giving the quality factor of about 9000.

The threshold power for the microring/microdisk structures was estimated from a light-light curve of the dominant mode. An example is presented in Figure 8 where a characteristic knee is clearly seen. In this particular case ($D = 7$ μm,

$d = 3.4$ µm) the threshold power is 0.37 mW. No correction was made to take into account partial light reflection from the surface or waste of the excitation power in the inner area of microring structures. Overall the threshold power at room temperature in different structures ranges from few tenths of mW to few mW. From one to three modes were usually observed in room-temperature lasing spectra (see right insert of Figure 8).

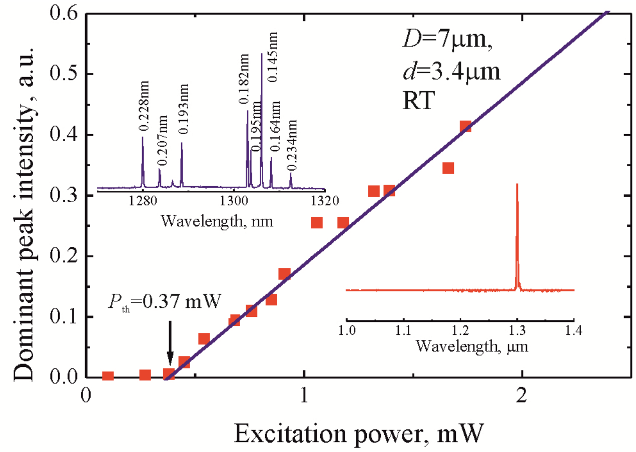

Figure 8. Intensity of the dominant mode against excitation power (symbols). Curve is a guide to the eye. Insert: luminescence spectrum below threshold (left) and above threshold (right).

Room-temperature threshold characteristics of the microstructures with different inner diameters were compared. In most cases the threshold power (absolute value) decreases by approximately 30-40% as the inner diameter increases from 0 (disk) to 0.3-0.6 D, see Figure 9. Further ring thinning results in rapid growth of the threshold. As for the effect of the outer diameter, the lowest threshold of 0.37-0.4 mW was found in microrings having an outer diameter of 6–7 µm. Both larger and smaller microrings demonstrate higher threshold power as shown in the insert of Figure 9.

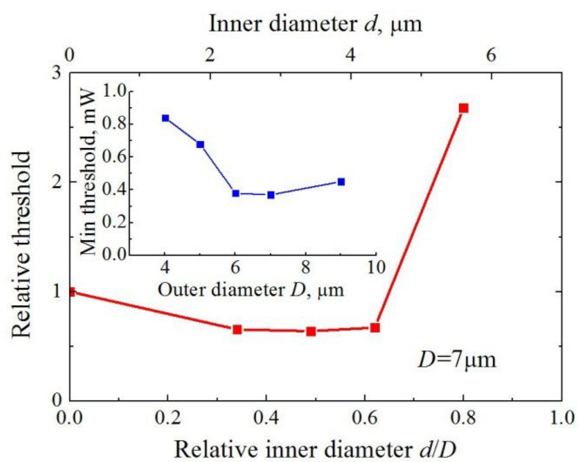

Figure 9. Room-temperature threshold (normalized to the threshold of the microdisk structure) as a function of inner diameter. Insert: the lowest threshold against the outer diameter.

3.5 High-temperature measurements

Threshold power increases super-exponentially with temperature. Around room temperature the characteristic temperature was estimated to be ~60–75 K. In most cases, lasing can be observed up to 80–90°C whereas the highest temperature of lasing was found to be as high as 107°C, Figure 10. To the best of our knowledge this is the highest temperature ever reported for 1.3μm QD MRLs. Below room temperature the threshold is nearly unchanged or even slightly increases. Temperature variation of the lasing wavelength is summarized in Figure 10. Spectral position of the ground-state optical transition of quantum-dot luminescence is also shown for comparison. It is seen that the lasing wavelength is quite stable (~0.05 nm/K) within relatively wide temperature intervals (e.g. from 20 to 40°C and then from 50 to 90°C) where a certain WGM mode remains the dominant one. Abrupt changes of the lasing wavelength (e.g. around 40-50 °C) are due to hopping of the dominant mode.

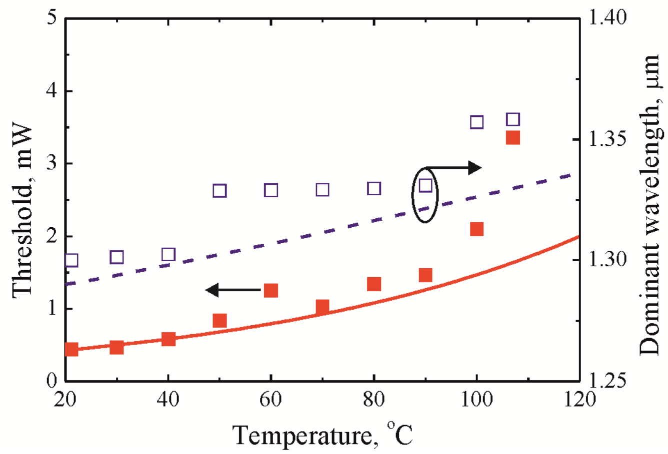

Figure 10. Temperature dependences of the threshold power (solid symbols) and wavelengths of the dominant mode (open symbols). QD ground-state optical transition against temperature (dashed curve) is also shown. Solid curve is exponential fit with T_0=65 K.

4. CONCLUSIONS

Quantum dot lasing structures of two sorts both emitting around 1.3 μm were studied: broad-area diode lasers and optically pumped microresonators.

Broad-area lasers were used for detailed investigation of the two-state lasing phenomenon and, in particular, quenching of the ground-state lasing emission that observed at high currents. It was demonstrated that the most probable reason for the GS lasing quenching is asymmetry of electrons and holes carrier distributions. Additionally, difference in capture rates of electrons and holes has to be taken into consideration. We also found that the GS-component reaches its maximum beyond the threshold of the two-state lasing and that different groups of QDs are responsible for GS- and ES1-lasing in the two-state lasing regime. Finally, we demonstrated that *p*-type modulation doping of QDs leads to noticeable suppression of the ES1-lasing thereby resulting in enhancement of peak power of the GS spectral component.

Microrings and microdisks of few micrometers in diameter were made by ion etching and selective oxidation with Q-factor of about 9000. Whispering gallery modes of second and third radial orders dominate the luminescence spectrum. Nearly single-mode lasing was observed at elevated temperatures. The lowest threshold (around 0.4 mW at RT) was found in microdisks of intermediate diameter (6-7 μm) with approximately 50% inner aperture. The highest temperature was found to be 107°C and the threshold was in mW-range.

ACKNOWLEDGEMENTS

The work is supported in different parts by Russian Ministry of Science and Education, Russian Foundation for Basic Research, Programs of Fundamental Studies of the Russian Academy of Sciences. NVK is thankful for support to Saint-Petersburg`s Committee on Science and Higher School.

REFERENCES

[1] Zhukov, A. E., Kovsh, A. R., Livshits, D. A., Ustinov, V. M. and Alferov, Zh. I., "Output power and its limitation in ridge-waveguide 1.3 μm wavelength quantum-dot lasers," Semicond. Sci. Technol. 18(8), 774-781 (2003).

[2] Markus, A., Chen, J. X., Gauthier-Lafaye, O., Provost, J.-G., Paranthoën, C. and Fiore, A., "Impact of intraband relaxation on the performance of a quantum-dot laser," IEEE J. Select. Topics Quantum Electron. 9(5), 1308-1314 (2003).

[3] Markus, A. and Fiore, A., "Modeling carrier dynamics in quantum-dot lasers," phys. stat. sol. (a) 201(2), 338–344 (2004).

[4] Ji, H.-M., Yang, T., Cao, Y.-L., Xu, P.-F., Gu, Y.-X. and Wang, Zh.-G., "Self-heating effect on the two-state lasing behaviors in 1.3-μm InAs–GaAs quantum-dot lasers," Jpn. J. Appl. Phys. 49(7), 072103 (2010).

[5] Sugawara, M., Hatori, N., Ebe, H., Ishida, M., Arakawa, Y., Akiyama, T., Otsubo, K. and Nakata, Y., "Modeling room-temperature lasing spectra of 1.3-μm self-assembled InAs/GaAs quantum-dot lasers: Homogeneous broadening of optical gain under current injection," J. Appl. Phys. 97(4), 043523 (2005).

[6] Liang, D., Fiorentino, M., Srinivasan, S., Bowers, J. E. and Beausoleil, R. G., "Low threshold electrically-pumped hybrid silicon microring laser," IEEE J. Selected Topics Quantum Electron., 17(6), 1528 - 1533 (2011).

[7] Ouyang, D., Ledentsov, N. N., Bimberg, D., Kovsh, A. R., Zhukov, A. E., Mikhrin S. S. and Ustinov, V. M., "High performance narrow stripe quantum-dot lasers with etched waveguide," Semicond. Sci. Technol. 18(12) L53-L54 (2003).

[8] Cao, H., Xu, J. Y., Xiang, W. H., Ma, Y., Chang, S.-H., Ho, S. T. and Solomon, G. S., "Optically pumped InAs quantum dot microdisk lasers," Appl. Phys. Lett. 76(24), 3519-3521 (2000).

[9] Ide, T., Baba, T., Tatebayashi, J., Iwamoto, S., Nakaoka, T. and Arakawa, Y., "Room temperature continuous wave lasing in InAs quantum-dot microdisks with air cladding," Opt. Express 13(5), 1615-1620 (2005).

[10] Munsch, M., Claudon, J., Malik, N. S., Gilbert, K., Grosse, P., Gerard, J.-M., Albert, F., Langer, F., Schlereth, T., Pieczarka, M. M., Hofling, S., Kamp, M., Forchel, A. and Reitzenstein, S., "Room temperature, continuous wave lasing in microcylinder and microring quantum dot laser diodes," Appl. Phys. Lett. 100(3), 031111 (2012).

[11] Viktorov, E. A., Mandel, P., Tanguy, Y., Houlihan, J. and Huyet, G., "Electron-hole asymmetry and two-state lasing in quantum dot lasers," Appl. Phys. Lett. 87(5), 053113 (2005).

[12] Fathpour, S., Mi, Z., Bhattacharya, P., Kovsh, A. R., Mikhrin, S. S., Krestnikov, I. L., Kozhukhov, A. V., and Ledentsov, N. N., "The role of Auger recombination in the temperature-dependent output characteristics ($T_0=\infty$) of p-doped 1.3 μm quantum dot lasers," Appl. Phys. Lett. 85(2), 5164-5166 (2004).